Energy Conversion and Management 156 (2018) 403–415

Contents lists available at ScienceDirect

Energy Conversion and Management

journal homepage: www.elsevier.com/locate/enconman

National and global wind resource assessment under six wind turbine installation scenarios

Christopher Jung*, Dirk Schindler, Jessica Laible

Environmental Meteorology, Albert-Ludwigs-University of Freiburg, Werthmannstrasse 10, D-79085 Freiburg, Germany

ARTICLE INFO

Keywords:
Wind resource
Wind energy yield
Capacity factor
Electricity consumption
ERA-20C

ABSTRACT

Based on ERA-20C data available for the period 2008–2010, the potential of six onshore wind turbine installation scenarios to cover current electricity consumption at the national and global scale was studied. The technical wind energy potential was estimated using the recently developed, highly accurate Burr-Generalized Extreme Value mixture distribution. The installation scenarios were evaluated by varying wind farm efficiency, the concentration of wind turbines, and wind turbine siting strategy for wind turbine densities of 1–25% of the land area. With the systematic installation of wind turbines at the national scale and international coordination of energy distribution, wind energy production could match current electricity consumption in the 2030s assuming a tenfold increase in current expansion rate. However, the results greatly differ from country to country mainly because of the meteorological potential, the total area available for wind turbine installation, and the population size. In industrialized countries such as China, France, Germany, and Japan, either low average annual wind energy yield or the large population prevents complete coverage of electricity consumption by wind energy at low and moderate wind turbine density. In developing countries including Ethiopia, Sudan or Kenia, where wind energy potential is high and electricity consumption is low, expansion of wind energy could greatly improve electricity supply. It was found that 98 countries could cover their current electricity consumption by an installed capacity of 0.0734 MW/km^2. This installed capacity enables 73 countries to cover even a 100% increase of the current electricity consumption. Based on the range of evaluated scenarios, it is possible to estimate the upper and lower bounds of the technical potential predefined by the applied wind turbine densities.

1. Introduction

Along with economic development, electricity consumption has steadily increased over the last decades [1]. In 1980, globally consumed electricity was 7,319 TW h/yr. Until 2014, global electricity consumption increased by 283%, reaching 20,715 TW h/yr [2]. The countries with the highest electricity consumption in 2014 were China (5,113 TW h/yr, including Hong Kong and Macau) and the USA (3,913 TW h/yr) (Fig. 1).

Currently, conventional fuels are predominately used to cover electricity consumption [3]. However, the utilization of conventional fuels is connected with greenhouse gas emissions, which drive climate change [4]. Furthermore, emissions of air pollutants pose human health risks [5]. In addition, anticipated peaking of fossil fuels requires finding appropriate substitutes such as renewable energies [6]. Renewable energies are vital sources of future energy helping to mitigate climate change [7]. They are clean, environmentally friendly, and health-compatible alternatives to fossil fuels [8].

Wind turbines convert kinetic energy contained in the wind first into mechanical and then into electrical energy [9]. Nowadays, wind turbine technology is considered to be matured and the costs of wind energy are low [10]. The current expansion rate of installed wind energy capacity (*IC*) is enormous. From 2001 to 2016, *IC* increased by 2,037% from 23,900 MW to 486,790 MW. In 2016, the highest wind energy capacity was installed in China (168,690 MW), the USA (82,184 MW), and Germany (50,018 MW). The corresponding installed capacities per area were 0.018 MW/km^2 in China, 0.009 MW/km^2 in the USA, and 0.1435 MW/km^2 in Germany [11].

The wind energy potential is typically divided into five categories which are hierarchically structured [12]: (1) the meteorological potential, which is the available wind resource, (2) the site potential, which excludes geographical unsuitable areas from the meteorological potential, (3) the technical potential, which takes the available wind energy technology into account, (4) the economic potential, which is defined as the technical potential that can be realized, and (5) the implementation potential which considers constraints and incentives

* Corresponding author.
E-mail address: christopher.jung@mail.unr.uni-freiburg.de (C. Jung).

https://doi.org/10.1016/j.enconman.2017.11.059
Received 30 August 2017; Received in revised form 17 November 2017; Accepted 19 November 2017
Available online 01 December 2017

Nomenclature

Acronyms

a.g.l.	above ground level
B-GEV	Burr-Generalized Extreme Value distribution
CanadaSC5	scenario 5 estimations for Canada
cdf	cumulative distribution function
epdf	empirical probability density function
pdf	probability density function
RussiaSC5	scenario 5 estimations for Russia
SC1-SC6	wind turbine installation scenario 1–6

Symbols

$\overline{P}$	mean wind power density (W/m^2)
$\overline{x}$	mean wind speed (m/s)
μ	location parameter of Generalized Extreme Value distribution
AEY	annual average wind energy yield (GW h/yr)
AEYC	annual average wind energy yield per country (TW h/yr)
AEYG	global annual average wind energy yield (TW h/yr)
APR	atmospheric pressure (Pa)
CF	capacity factor
EC	electricity consumption (TW h/yr)
f	probability density function
F	cumulative distribution function
G	atmospheric gas constant (J/kg K)
IC	installed wind energy capacity (MW)
K	total number of countries
k	country
MAPE	mean absolute percentage error (%)
n	number of hours in a year (h)
P	power (W)
R^2	coefficient of determination
S	share of wind energy covering electricity consumption of 2014
SR	scenario ratio *AEYC*(SC1)/*AEYC*(SC6)
T	temperature (K)
u	zonal wind vector component (m/s)
v	meridional wind vector component (m/s)
WFE	wind farm efficiency
WTAC	wind turbine area per country (km^2)
WTD	wind turbine density per country (%)
WTN	number of wind turbines at *WTAC* grid cells (wind turbines/km^2)
WTT	wind turbine availability
x	wind speed (m/s)
z	grid cell (1 km^2)
η	scale parameter of Generalized Extreme Value distribution
ι	shape parameter of Generalized Extreme Value distribution
o	first shape parameter of Burr distribution
ρ	air density (kg/m^3)
σ	scale parameter of Burr distribution
χ	second shape parameter of Burr distribution
ω	mixing parameter of Burr-Generalized Extreme Value distribution

Subscripts

0	average conditions
a	air
B	Burr
emp	empirical
GEV	Generalized Extreme Value
W	wind turbine
z	grid cell

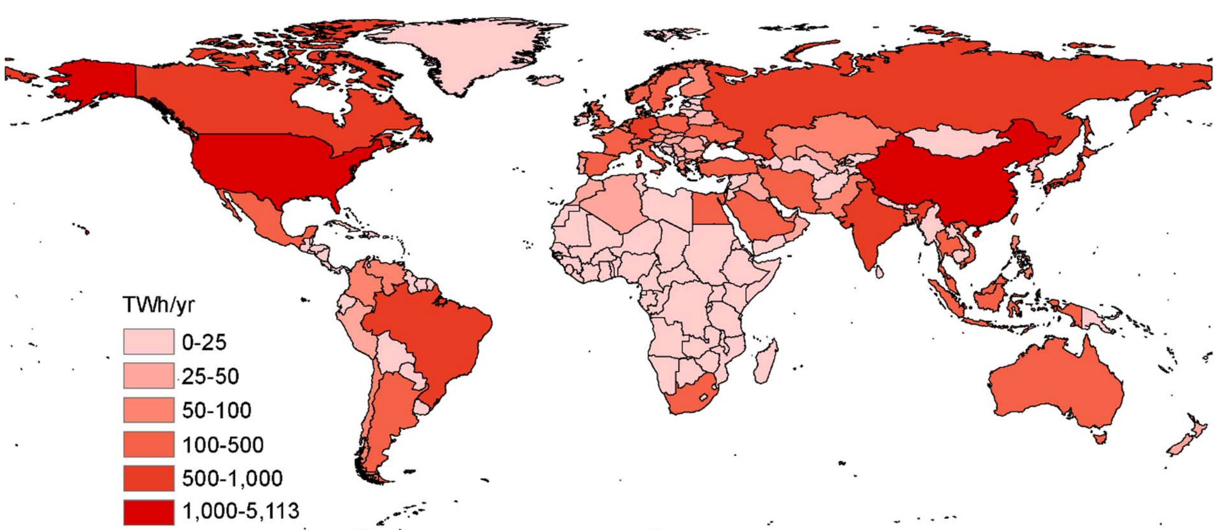

Fig. 1. Electricity consumption in 2014 [2].

that determine the time required to install wind turbines.

The global technical potential of wind energy has been investigated in several previous studies. Based on approach and applied specifications, the obtained results vary greatly among these studies. For instance, in a bottom-up study, it was estimated that a dense network of 2.5 MW onshore wind turbines could generate 1,100 PW h/yr electrical energy [13]. In a top-down study, the estimated electricity generation was lower amounting to 158–596 PW h/yr [14]. In that study, it was argued that each wind turbine extracts kinetic energy from the atmosphere, which reduces the overall extractability of kinetic energy and wind speed (x) on a large scale [15]. However, it has been demonstrated that this effect becomes important only at magnitudes that clearly surpass current electricity consumption or even primary energy consumption [16].

Previous studies mainly focused on the total extractable wind energy. However, real-world expansion of wind energy utilization is limited by a number of factors that will not allow exploiting the available amount of extractable wind energy in a reasonable period of time. Among the limiting factors are costs arising from the installation, long-distance electricity transmission, and storage [17]. Furthermore, concerns of the local population often complicate wind turbine installation [18]. Therefore, the focus of this study is not on estimating the maximum amount of extractable kinetic energy, but on projecting the effects of improved efficiency of wind energy utilization. To demonstrate these effects at national and global scale, six installation scenarios with various wind energy expansion rates were developed. They are intended to show possible paths towards covering current national and global electricity consumption by onshore wind energy. The scenarios have a clear meteorological and geographical focus taking the spatiotemporal variability of wind speed, wind turbine siting strategy, the concentration of wind turbines, area consumption, and wind farm efficiency into account.

The goals of this investigation are (1) assessing onshore wind turbine density required to cover current national and global electricity consumption considering various wind turbine installation scenarios, and (2) quantifying influences of the spatial distribution of wind turbines on the wind energy yield.

2. Methodology

2.1. Overview

The assessment of the national and global onshore technical wind energy potential included the following steps (Fig. 2): (1) preparation and analysis of wind speed time series on a global grid, (2) estimation of grid cell-specific empirical probability density functions (epdf) of wind speed at hub height and fitting of the Burr-Generalized Extreme Value distribution (B-GEV) to epdf, (3) computation of grid cell-specific average annual wind energy yield (*AEY*) by applying five power curves, (4) identification and exclusion of unsuitable areas by considering geographic constraints, (5) assessment of *AEY* on the national (*AEYC*) and (6) on the global scale (*AEYG*) by applying six different wind turbine installation scenarios (SC1-SC6) for different wind turbine densities (*WTD*).

2.2. Wind speed data

The horizontal wind vector components (u (zonal), v (meridional)) of ERA-20C data [19] were used to calculate wind speed at 100 m above ground level (a.g.l.) on the global scale excluding the Antarctica according to

$$x = \sqrt{u^2 + v^2}. \tag{1}$$

Wind speed values were computed for the period 01-01-2008 to 12-31-2010 every three hours [20]. The spatial resolution of the x values was 0.25° × 0.25°.

The ERA-20C data is based on a coupled atmosphere/land-surface/ocean-waves model. It simulates the weather by assimilating up to 3.6 million quality controlled surface observations per month in the period 1900–2010. The atmosphere is described at 91 vertical levels, between the surface and the 0.01 hPa pressure level [21]. The most relevant ERA-20C data for this study are the wind vector components in 100 m a.g.l. which is a typical wind turbine hub height.

2.3. Distribution fitting

Since epdf only represents a sample of x, a theoretical distribution was fitted to x epdf to represent the entire population. The proper choice of theoretical distributions for fitting x epdf is crucial for error reduction in wind resource estimation [22]. In a previous study, it was found that the seven-parameter B-GEV is the most suitable distribution for the vast majority of onshore wind speed regimes [23].

The first part of B-GEV is the three parameter Burr distribution with its probability density function (pdf) being [24]

$$f_B(x;\sigma,\chi,o) = \frac{o\chi\left(\frac{x}{\sigma}\right)^{o-1}}{\sigma\left[1+\left(\frac{x}{\sigma}\right)^{o}\right]^{\chi+1}} \tag{2}$$

where σ is the scale parameter, o and χ are the shape parameters. The cumulative distribution function (cdf) of the Burr distribution is given by [24]

$$F_B(x;\sigma,\chi,o) = 1-\left[1+\left(\frac{x}{\sigma}\right)^{o}\right]^{-\chi}. \tag{3}$$

The Generalized Extreme Value distribution, which is the second part of B-GEV, is defined by one location parameter (μ), one scale parameter (η), and one shape parameter (ι). Its pdf and cdf are given by [24]

$$f_{GEV}(x;\mu,\eta,\iota) = \frac{1}{\eta}\left[1-\frac{\iota}{\eta}(x-\mu)\right]^{\frac{1}{\iota}-1}\exp\left\{-\left[1-\frac{\iota}{\eta}(x-\mu)\right]^{\frac{1}{\iota}}\right\} \tag{4}$$

and

$$F_{GEV}(x;\mu,\eta,\iota) = \exp\left\{-\left[1+\iota\frac{(x-\mu)}{\eta}\right]^{\frac{-1}{\iota}}\right\}. \tag{5}$$

By mixing both Burr and Generalized Extreme Value distributions, B-GEV is formed with pdf and cdf being [24]

$$f_{B,GEV}(x;\omega,\sigma,\chi,o,\mu,\eta,\iota) = \omega f_B(x;\sigma,\chi,o) + (1-\omega)f_{GEV}(x;\mu,\eta,\iota) \tag{6}$$

and

$$F_{B,GEV}(x;\omega,\sigma,\chi,o,\mu,\eta,\iota) = \omega F_B(x;\sigma,\chi,o) + (1-\omega)F_{GEV}(x;\mu,\eta,\iota) \tag{7}$$

where ω is the mixing parameter. Parameter estimation of B-GEV was carried out by applying the least squares estimation method using the Levenberg-Marquardt algorithm [25].

2.4. Calculation of grid cell-specific average annual wind energy yield

The grid cell-specific average annual wind energy yield was estimated for average air density conditions ($\rho_O = 1.225\,\text{kg/m}^3$) using B-

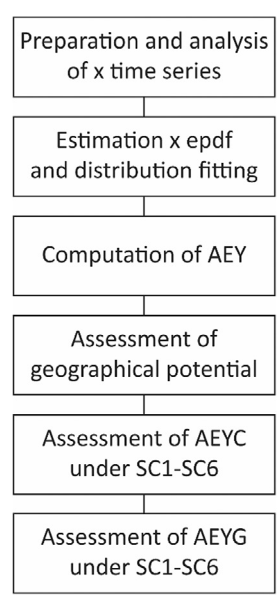

Fig. 2. Methodology applied to assess the national (*AEYC*) and global (*AEYG*) onshore technical wind energy potential.

GEV [12]:

$$AEY_{\rho_0} = n \int_0^{\infty} P_W(x) f_{B,GEV}(x) dx \tag{8}$$

where n is the number of hours in a year (8760 h) and P_W is the power output of a wind turbine. The ρ_0 value is representative for air temperature (T_a) of 15 °C and atmospheric pressure (APR) of 1000 hPa. The P_W values are typically described by wind turbine-specific power curves that share the following common characteristics [26]: the cut-in speed at which the wind turbine starts to generate usable power, the rated output speed at which the maximum output power is generated, and the cut-out speed at which the wind turbine shuts down in order to prevent damage. In this study, $AEY_{\rho 0}$ was calculated for five different wind turbine types and averaged. All evaluated wind turbine types are available in configurations with a hub height of ~100 m a.g.l. The selected power curves were taken from modern wind turbine types of some of the world's largest manufacturers. The power curves' characteristics are summarized in Table 1. The rated output power of the wind turbines varies between 2.5 and 5.0 MW.

To account for variations of ρ, its influence on $AEY_{\rho 0}$ was corrected. This was done by calculating the grid cell-specific average air density from ERA-20C data according to [12]:

$$\rho = \frac{APR}{G \cdot T_a} \tag{9}$$

with G being the atmospheric gas constant (287.058 J/kg K). Then, AEY was calculated as [12]:

$$AEY = AEY_{\rho_0} \cdot \left(\frac{\rho}{\rho_0}\right) \tag{10}$$

The efficiency of wind energy utilization was further assessed by the capacity factor (CF) [32]:

$$CF = \frac{AEY/8760}{\text{rated output power}} \tag{11}$$

and the mean wind power density ($\overline{P}$) [33]

$$\overline{P} = \frac{1}{2} \int_0^{\infty} \rho x^3 f_{B,GEV}(x) dx. \tag{12}$$

2.5. Geographic constraints

Compared with onshore wind energy, the current absolute expansion of offshore wind energy is low because of higher costs for construction, grid connection, and operation. Thus, it is very reasonable to expect that in most countries wind turbines are first sited onshore and then offshore. However, not all land areas are suitable for wind turbine installation. As recommended in a previous study [13], ice-covered regions, lakes, urban areas, wetlands, and evergreen forests were excluded from global and national annual average wind energy yield assessment. These exclusion areas were derived from data (resolution: 1 km × 1 km) provided by the International Geosphere-Biosphere Programme [34]. Furthermore, conservation areas were excluded using vector data from the protected planet project managed by the United Nations Environment Programme's World Conservation Monitoring Centre [35]. The Global Multi-resolution Terrain Elevation Data 2010 were used for calculation of slope values (resolution: 1 km × 1 km) [36]. Areas where slope exceeds 10° were excluded from the assessment [37].

Since permafrost areas complicate wind turbine installation [38] and can lead to a substantial reduction of national and global annual average wind energy yield, these areas were excluded in SC5. The resulting decrease in national and global annual average wind energy yield was compared to SC1-SC4 and SC6. The Global Permafrost Zonation Index Map [39] was used to identify the permafrost areas (resolution: 1 km × 1 km). To harmonize the resolution of all data, AEY was converted to a 1 km × 1 km resolution grid yielding AEY_z (z is the grid cell index). All data were prepared using ArcGIS® 10.2 software (Esri, Redlands, CA, USA).

2.6. Calculation of average annual wind energy yield

To calculate $AEYC$ from AEY_z, several aspects have to be considered: First, wind turbines are often arranged in wind farms at sites where AEY is high. This results in a concentration of wind turbines at certain grid cells and in an uneven wind turbine distribution at national and global scale. The concentration of wind turbines reduces AEY due to wake effects [40] which was taken into account by the wind farm efficiency (WFE) [41]. Second, wind turbines are not continuously in operation, which was quantified by the wind turbine availability (WTT). A typical WTT value is 0.97 [42].

Using WFE and WTT, $AEYC$ was calculated as

$$AEYC = \sum_{z=1}^{WTAC} AEY_z \cdot WTN \cdot WFE \cdot WTT \tag{13}$$

with $WTAC$ being the wind turbine area per country, which is defined as the number of grid cells where wind turbines are located and WTN is the number of wind turbines at each of these grid cells.

The number of wind turbines per country was defined as

$$\text{Wind turbines per country} = \text{Area size} \cdot WTD. \tag{14}$$

Subsequently, $WTAC$ was quantified as

$$WTAC = \frac{\text{Wind turbines per country}}{WTN}. \tag{15}$$

To obtain the grid cells used in (13), country-specific AEY_z values were arranged in descending order ($z = \max(AEY_z),...,\min(AEY_z)$).

Global annual average wind energy yield was calculated according to

$$AEYG = \sum_{k=1}^{K} AEYC_k \tag{16}$$

with $AEYC_k$ being the average annual wind energy yield for country k, and K is the total number of countries. Six wind turbine installation scenarios account for variation of WTN, WFE, and WTD which represents the relative density of wind turbines per km^2 (in %) of a country (Table 2).

The maximum number of wind turbines per km^2, considering the rotor diameters of the evaluated wind turbine types, was limited to $WTN = 2$ to minimize wake effects [37]. The scenarios SC2 and SC4 assume that wind turbines are sited with a higher density ($WTN = 2$), whereas the other scenarios assume that wind turbines are sited with a lower density ($WTN = 1$). Variations in wake effect were considered by $WFE = 0.90$ and $WFE = 0.95$ under SC1-SC5. In scenarios where WFE is 0.95, wind farms are designed to minimize wake effects. In SC1-SC5, wind turbines were sited with a systematic approach. SC6 was developed by randomly arranging AEY_z on the national scale, i.e. there is no systematic wind resource assessment and wind turbine siting. The

Table 1
Properties of the evaluated power curves.

Wind turbine type	Cut-in speed	Rated output speed	Rated output power	Cut-out speed
G128 [27]	2.0 m/s	14.0 m/s	5.00 MW	27.0 m/s
E-126 EP4 [28]	3.0 m/s	13.5 m/s	4.20 MW	25.0 m/s
V112-3.45 MW [29]	3.0 m/s	13.0 m/s	3.45 MW	25.0 m/s
SWT-3.2-113 [30]	3.0 m/s	12.5 m/s	3.20 MW	25.0 m/s
Vensys 100 [31]	3.0 m/s	11.0 m/s	2.50 MW	25.0 m/s

Table 2
Evaluated wind turbine installation scenarios (SC) with wind turbine number (*WTN*), wind farm efficiency (*WFE*), and wind turbine density (*WTD*).

Scenario	*WTN*	*WFE*	*WTD* (%)	Siting strategy
SC1	1	0.95	1–25	Systematic
SC2	2	0.95	1–25	Systematic
SC3	1	0.90	1–25	Systematic
SC4	2	0.90	1–25	Systematic
SC5	1	0.95	1–25	Systematic, excluding permafrost areas
SC6	1	1.00	1–25	Random

effects of the exclusion of permafrost areas on *AEYC* and *AEYG* were assessed in SC5. All wind turbine installation scenarios were evaluated for an expansion between $WTD = 1\%$ and $WTD = 25\%$.

The potential to cover current electricity consumption (*EC*) under SC1-SC6 was calculated by

$$S = \frac{AEYC}{EC}. \tag{17}$$

To quantify the difference between systematic and random wind turbine siting, the scenario ratio

$$SR = \frac{AEYC(SC1)}{AEYC(SC6)} \tag{18}$$

was calculated.

Since it is not possible to present results for all evaluated countries in the paper, some countries were chosen as an example. For these countries results on the estimated quantities are presented and discussed in the following sections. A comprehensive country-specific summary of all evaluated scenarios and wind turbine densities (*AEYC*) is provided in Tables S1–S6 (supporting information).

3. Results and discussion

3.1. Meteorological potential

The mean onshore wind speed at 100 m a.g.l. ($\overline{x}$) is shown in Fig. 3a. The average of all $\overline{x}$ values is 4.9 m/s. At 7.6% of the land surface, $\overline{x}$ exceeds 7.0 m/s. These areas, which offer a great meteorological potential, are mainly located in Greenland, the southern tip of South America, the North Sea coast, Western Sahara, Chad, Somalia, the Midwest of the USA, northern parts of Canada and Russia, and the southwest of Australia. At 12.6% of the land surface, $\overline{x}$ values below the typical cut-in speed ($\overline{x} \leqslant 3.0 m/s$) occur. These low $\overline{x}$ values can be found mainly in areas where surface roughness is high due to orographic sheltering (e.g. the Alps, the Himalaya, Andes Mountains) or due to the occurrence of tropical forests (e.g. Amazon Basin, Central Africa). In countries with complex terrain, where orographic features locally modify wind speed, it is reasonable to assume that actual wind speed at exposed mountain tops exceeds ERA-20C wind speed.

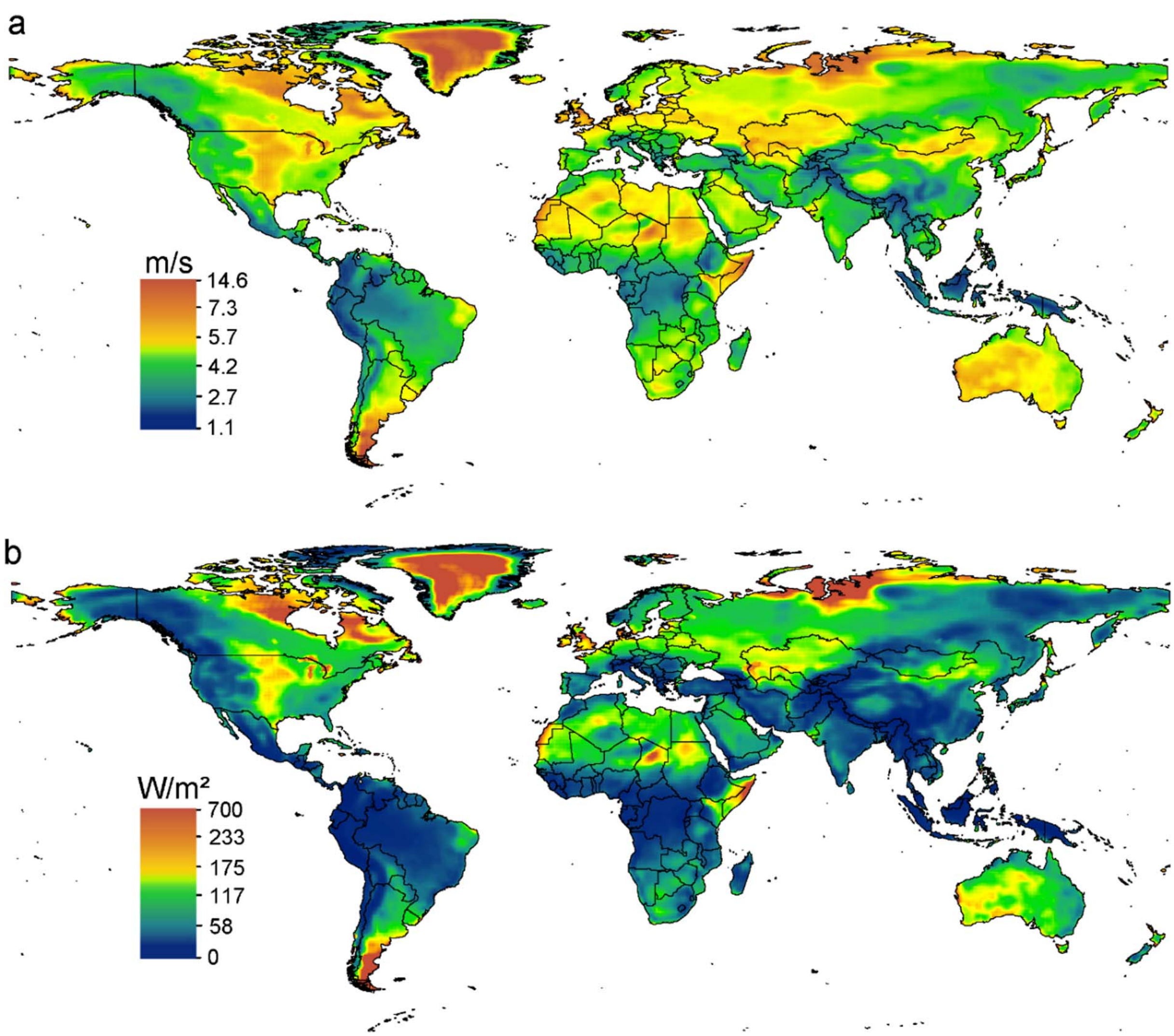

Fig. 3. (a) Mean wind speed at 100 m a.g.l. ($\overline{x}$) and (b) mean wind power density at 100 m a.g.l. ($\overline{P}$) without any geographic constraints being considered.

Due to the cubic increase of $\overline{P}$ as a function of $\overline{x}$, a rather small increase of $\overline{x}$ results in a large growth in $\overline{P}$ (Fig. 3b). In contrast, the effect of ρ on $\overline{P}$ is comparatively low. However, in mountainous regions, the decrease of ρ results in lower $\overline{P}$. Overall, at 34.1% of the land surface, $\overline{P}$ exceeds 100 W/m^2 which is considered sufficient for wind energy utilization [12]. From a meteorological point of view, these areas are generally suitable for wind turbine installation.

In the Midwest of the USA, $\overline{P}$ is around 200 W/m^2 over extensive areas, indicating a good meteorological potential. In China, sufficiently high wind speeds can be found predominantly in the northeast towards the Mongolian border. Areas with a great wind resource ($\overline{P}$ ~ 700 W/m^2) can be found on the Falkland Islands and in the Tierra del Fuego at the southern tip of South America. The west wind drift in the mid-southern latitudes determines the wind resource in these regions.

3.2. Goodness-of-fit evaluation of B-GEV

In Fig. 4, epdf and B-GEV pdf are shown for four different wind speed regimes occurring at a grid cell in the USA (Fig. 4a), China (Fig. 4b), Argentina (Fig. 4c), and Western Sahara (Fig. 4d). The grid cells located in the USA and China were chosen because these countries are the biggest electricity consumers. The grid cells located in Argentina and Western Sahara were chosen due to their great meteorological potential. Although the statistical moments greatly differ among the four wind speed regimes, B-GEV fits all four epdf very accurately.

To evaluate the goodness-of-fit of B-GEV at all grid cells, *AEY* estimated by B-GEV is plotted against empirical *AEY* (AEY_{emp}) in Fig. 5. The coefficient of determination is very high (R^2 = 0.9999) and the mean absolute percentage error is low (*MAPE* = 1.2%), both indicating an excellent fitting accuracy of B-GEV.

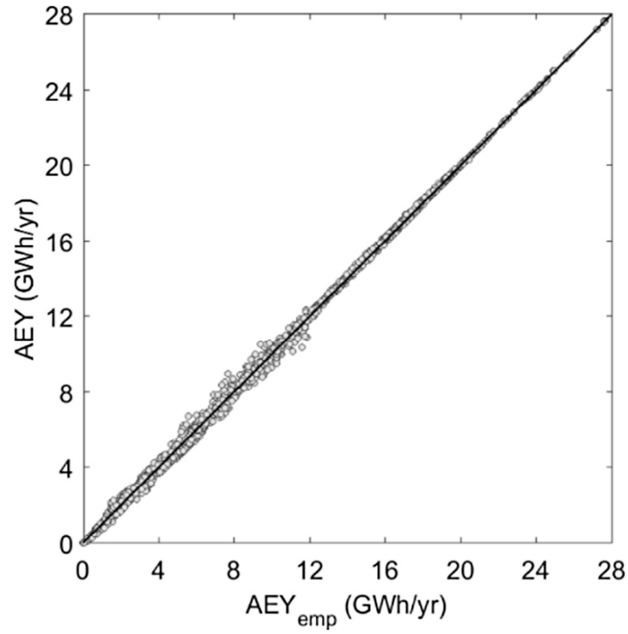

Fig. 5. Empirical annual average wind energy yield (AEY_{emp}) plotted against average annual wind energy yield estimated by B-GEV (*AEY*).

3.3. Technical wind energy potential

Fig. 6a illustrates the global AEY_z pattern including permafrost areas. According to that, 63.6% of the total land area are suitable for wind turbine installation. In these areas, mean AEY_z is 4.9 GW h/yr. At 7.8% of the areas suitable for wind turbine installation, AEY_z exceeds

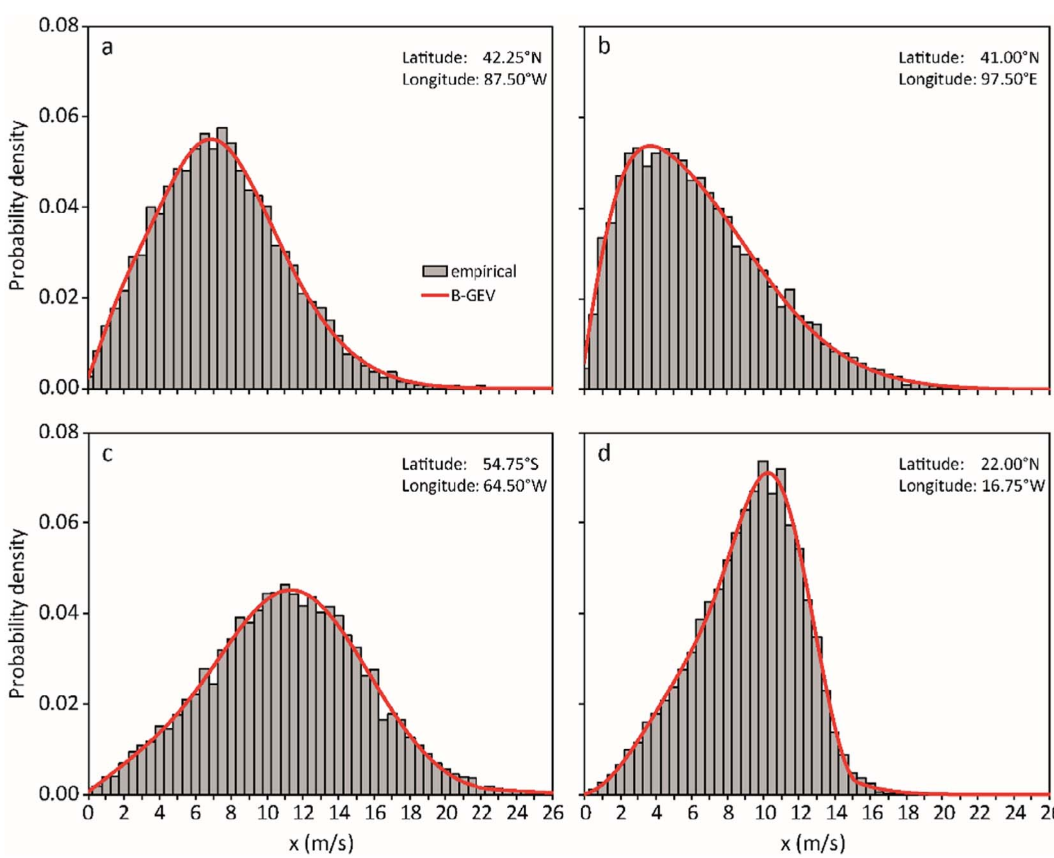

Fig. 4. Probability density functions of Burr-Generalized Extreme Value distribution (B-GEV) fitted to empirical probability density functions (epdf) of wind speed (*x*) related to grid cells in (a) the USA, (b) China, (c) Argentina, and (d) Western Sahara.

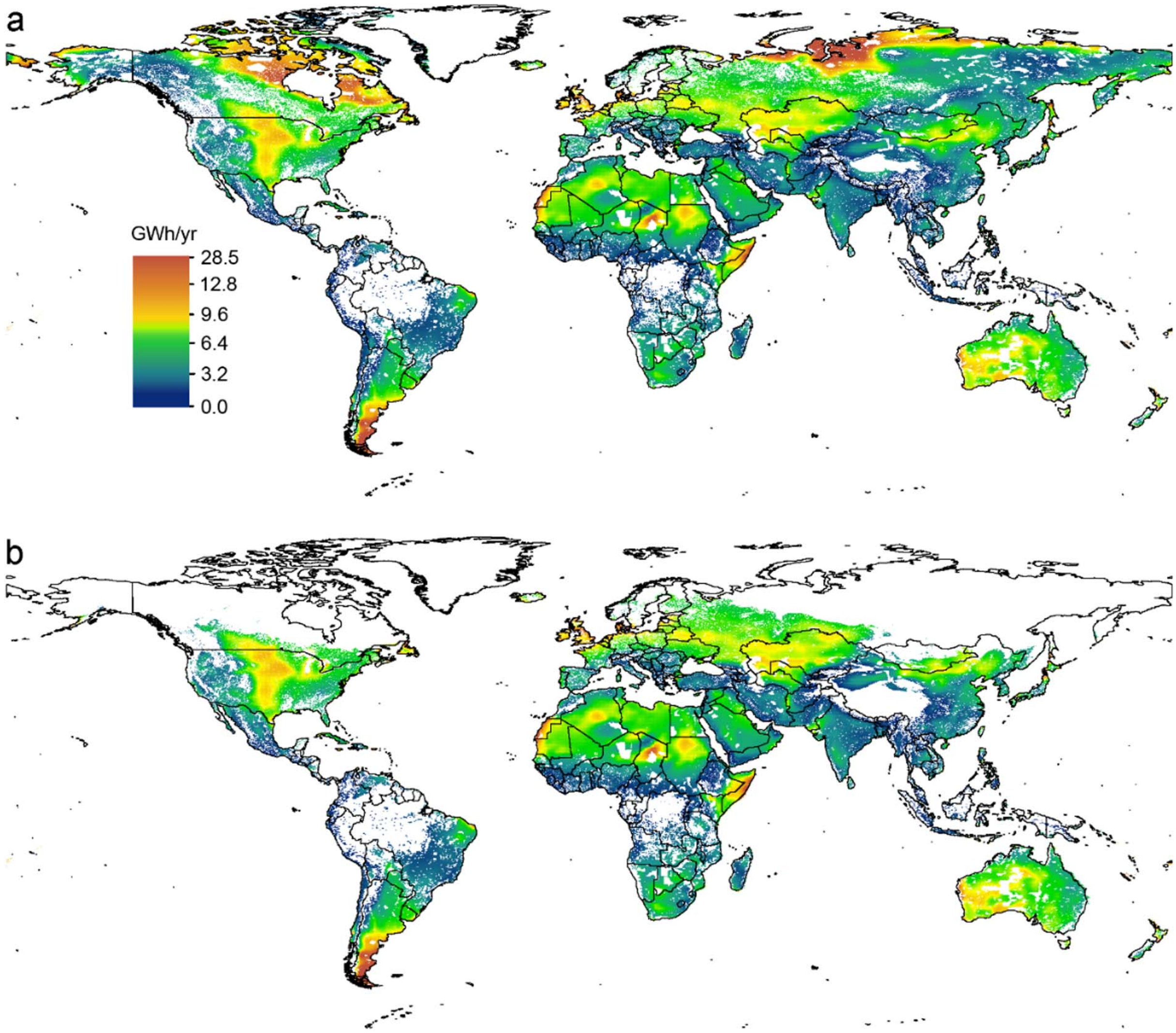

Fig. 6. Grid cell-related average annual wind energy yield (AEY_z) (a) including and (b) excluding permafrost areas.

10.0 GW h/yr. The Tierra del Fuego or the Midwest of the USA where the meteorological potential is good to great are only slightly affected by geographic constraints. Although the meteorological potential of Greenland is great, wind turbines cannot be installed due to extensive permanent snow and ice cover.

When permafrost areas are excluded from the AEY_z estimation, suitable areas decrease to 51.7% of the total land area (Fig. 6b) with the greatest area loss occurring in the northern parts of Russia and Canada. Other areas lost to permafrost are mainly located in Alaska, China, Scandinavia, and high mountain ranges. In the non-restricted areas, mean AEY_z is 4.8 GW h/yr.

3.4. Wind turbine installation scenarios

Fig. 7a illustrates annual average wind energy yield per country under SC1 with WTD = 2%. Under this scenario and wind turbine density, the wind energy potential in Russia is abundant ($AEYC$ = 5,024 TW h/yr). Canada ($AEYC$ = 2,762 GW h/yr) and the USA (2,115 TW h/yr) also have great wind resource. In total, 40 countries could generate more than 100 TW h/yr of electrical energy from kinetic energy contained in the wind. Summing up annual average wind energy yield per country of the 28 European Union countries including Great Britain yields 886 TW h/yr. This amount is less than $AEYC$ estimated for China (1,629 TW h/yr). In the North African countries such as Libya and Algeria, substantially more electrical energy could be generated from the wind than in countries which are mainly covered by tropical forests and where $AEYC$ is low. On the global scale, AEY amounts to 25,648 TW h/yr. Based on the results of this study and leaving the economic and implementation restrictions out of consideration, 98 countries could completely (S = 100%) cover their current electricity consumption (Fig. 7b). When electricity generated from the wind would be systematically allocated, global S would be 123.8%.

Since electricity consumption is low and annual average wind energy yield per country is high, many African countries could completely cover current electricity consumption by wind energy. Therefore, the installation of a limited number of wind turbines could greatly improve electricity supply in areas with no or no permanent access to electricity [43]. In the USA and China, S is 54.1% and 31.9%. Very low S values were estimated for the rather small European countries Switzerland (3.4%), Belgium (8.1%), and the Netherlands (8.4%).

Under SC1 and WTD = 2%, the combination of high $AEYC$/km^2 and low population density results in high wind energy production per capita. This combination is especially given in Argentina, Canada, and Russia (Fig. 8). Excluding permafrost areas, the Russian $AEYC$ = 35.0 MW h/yr/per capita would decrease to 20.7 MW h/yr/per capita (RussiaSC5). A distinct permafrost-related decrease of $AEYC$ from 76.9 MW h/yr/per capita to 57.3 MW h/yr/per capita is also estimated for Canada (CanadaSC5). Even though the electricity consumption in Russia and Canada is high, both countries could cover

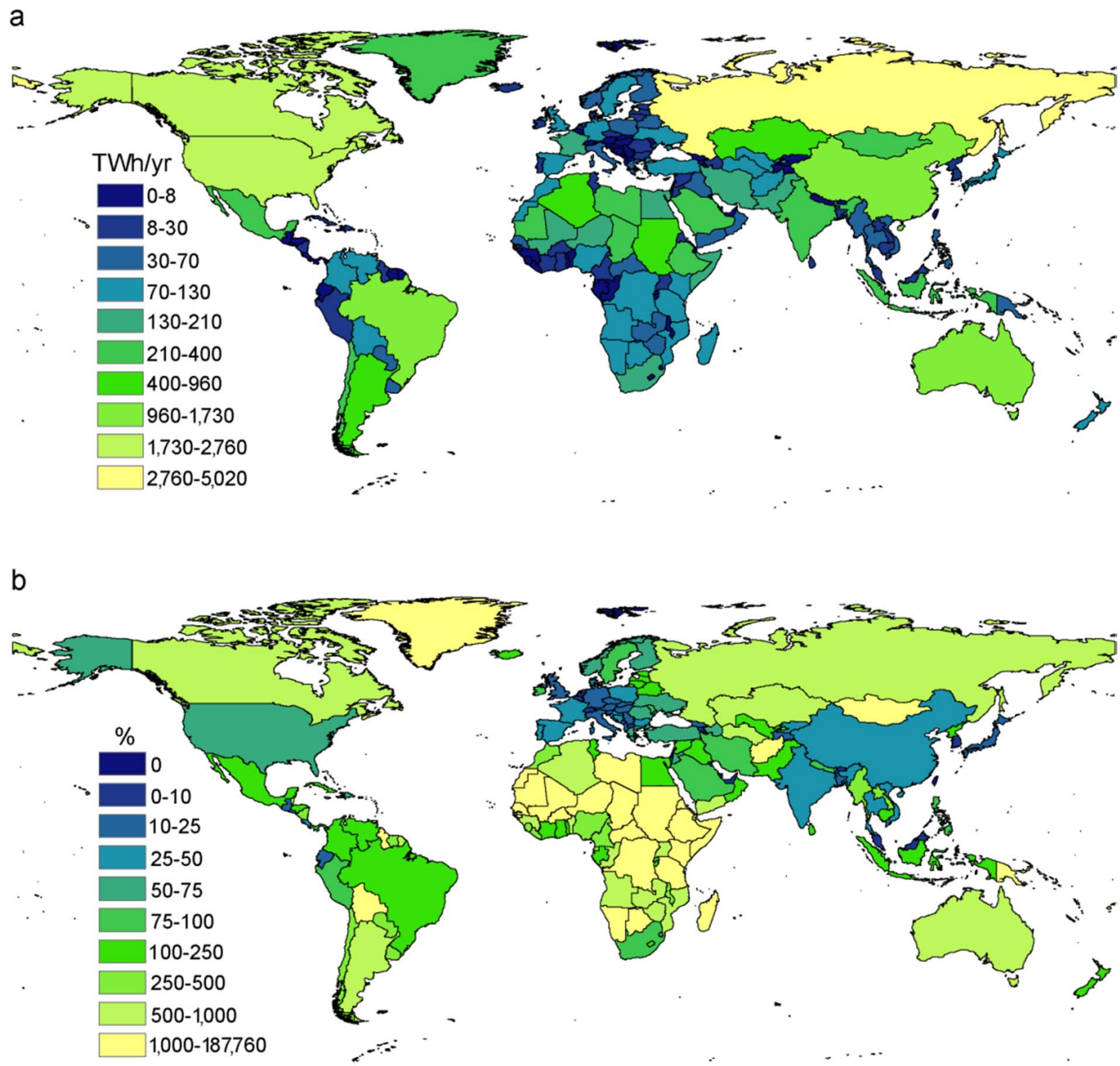

Fig. 7. (a) Annual average wind energy yield per country (*AEYC*) and (b) potential to cover current electricity consumption (*EC*) by wind energy (*S*) under scenario 1 (SC1) assuming a wind turbine density (*WTD*) of 2%.

electricity consumption many times over by systematically utilizing wind energy. On the other hand, in China, France, Germany, and Japan, either low $AEYC/\text{km}^2$ or the large population prevents complete coverage of electricity consumption by wind energy. In Ethiopia, Sudan or Kenya where *AEYC* per capita is high and electricity consumption is low there is a great potential that expansion of wind energy could improve electricity supply. Although *AEYC* is below $100\ \text{MW h/yr/km}^2$ in Uganda, Nigeria, Myanmar, and Ghana, it is sufficient to completely cover national electricity consumption.

The presented results demonstrate that the quantification of wind energy yield strongly depends on the reference quantity. Due to low electricity consumption and good wind resource ($> 200\ \text{W/m}^2$), wind energy is a feasible option for covering current and future electricity consumption in many African countries.

With its high population density and limited wind energy yield, Bangladesh has the lowest *AEYC* per capita of the 50 presented countries. Despite low electricity consumption per capita, in Nepal and Bangladesh, electricity consumption cannot be covered by wind energy because $AEYC < 100\ \text{MW h/yr/km}^2$.

The country-specific estimates of *WTD* under SC1 with $S \geq 100\%$ are presented in Fig. 9. In most African countries as well as in Canada, Russia, Brazil, Argentina, and Australia, $WTD \leq 1\%$ could result in $AEYC = EC$. In Mexico, Venezuela, Saudi Arabia, and South Africa, $2\% < WTD < 5\%$ is required to cover electricity consumption. In Italy, Japan, South Korea, and the Netherlands, $WTD > 25\%$ is required to cover electricity consumption.

Fig. 10a displays global annual average wind energy yield and share of wind energy covering electricity consumption of 2014 under SC1-SC6 as a function of wind turbine density and installed capacity. Under SC1-SC5, assuming $WTD = 2\%$ and $IC = 10.8$ TW, current global electricity consumption could be easily covered. Anticipating a continues growth of global electricity consumption over the next decades, a one and a half increase of the current electricity consumption ($S = 150\%$) will be covered at $WTD = 2.5\%$ and $IC = 13.5$ TW. At the current rate of increase of electricity consumption [2], $S = 150\%$ is reached in the 2030s. Even a sevenfold increase ($S = 700\%$) of current electricity consumption could be covered under all scenarios by $WTD < 25\%$.

An expansion rate equal to ten times the current expansion rate (~ 0.58 TW/yr) is required to cover electricity consumption between the early 2030s (SC1-SC5) and the mid-2040s (SC6). Assuming that

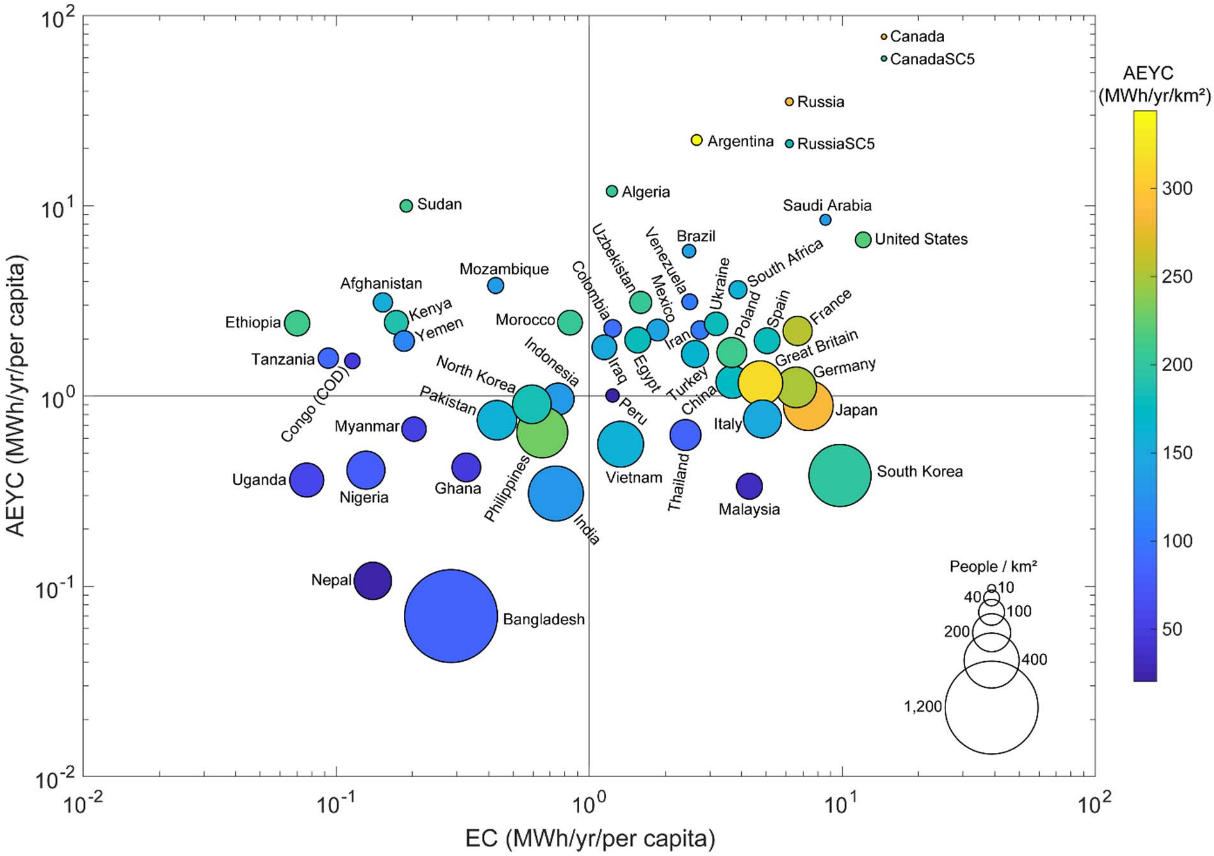

Fig. 8. Annual average wind energy yield per country (*AEYC*) per capita, electricity consumption (*EC*) per capita, *AEYC* per km² (bubble color) under scenario 1 (SC1) assuming a wind turbine density (*WTD*) of 2%. The bubble size classifies population density for the 50 countries with the highest total population. Results under scenario 5 calculations are shown for Canada (CanadaSC5) and Russia (RussiaSC5).

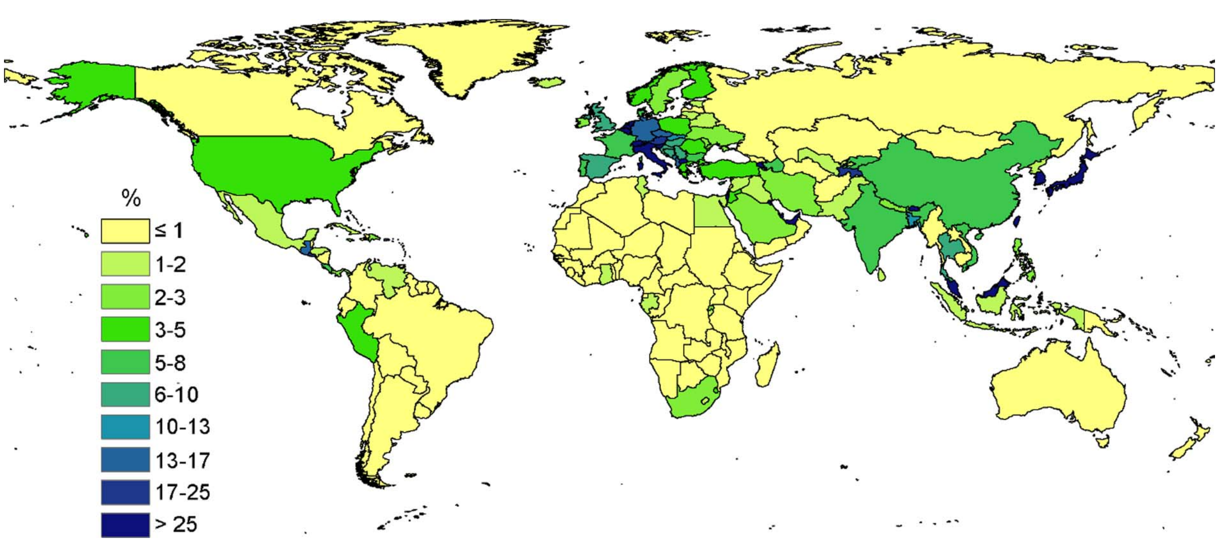

Fig. 9. Wind turbine density (*WTD*) at which country-specific average annual wind energy yield (*AEYC*) equals electricity consumption (*EC*) of 2014.

electricity consumption also increases over the next decades, it can be expected that electricity consumption coverage would occur even at a later time. The great differences between the curves representing SC1-SC6 emphasize the need for systematic wind turbine siting at national and global scale to ensure efficient wind energy utilization.

Assuming $WTD = 4\%$ and $IC = 1.4$ TW for the USA results in $59\% \leq S \leq 108\%$ for SC1-SC6 (Fig. 10b). If $WTD = 10\%$ and $IC = 3.5$ TW, S increases by 147% under SC6 and by 256% under SC2. The corresponding *AEYC* for these wind turbine densities vary between 5,759 TW h/yr and 10,020 TW h/yr.

Covering electricity consumption by wind energy in China requires greater efforts than in the USA (Fig. 10c). For $WTD = 7\%$ and $IC = 2.4$ TW, S varies between 31% (SC6) and 108% (SC2). Furthermore, a systematic siting of wind turbines has a greater effect on *AEYC* and S than in the USA.

In Germany, a country which already has installed a large number of wind turbines, wind turbine density and installed capacity would have to be at least 14% and 0.18 TW (SC2) to cover electricity

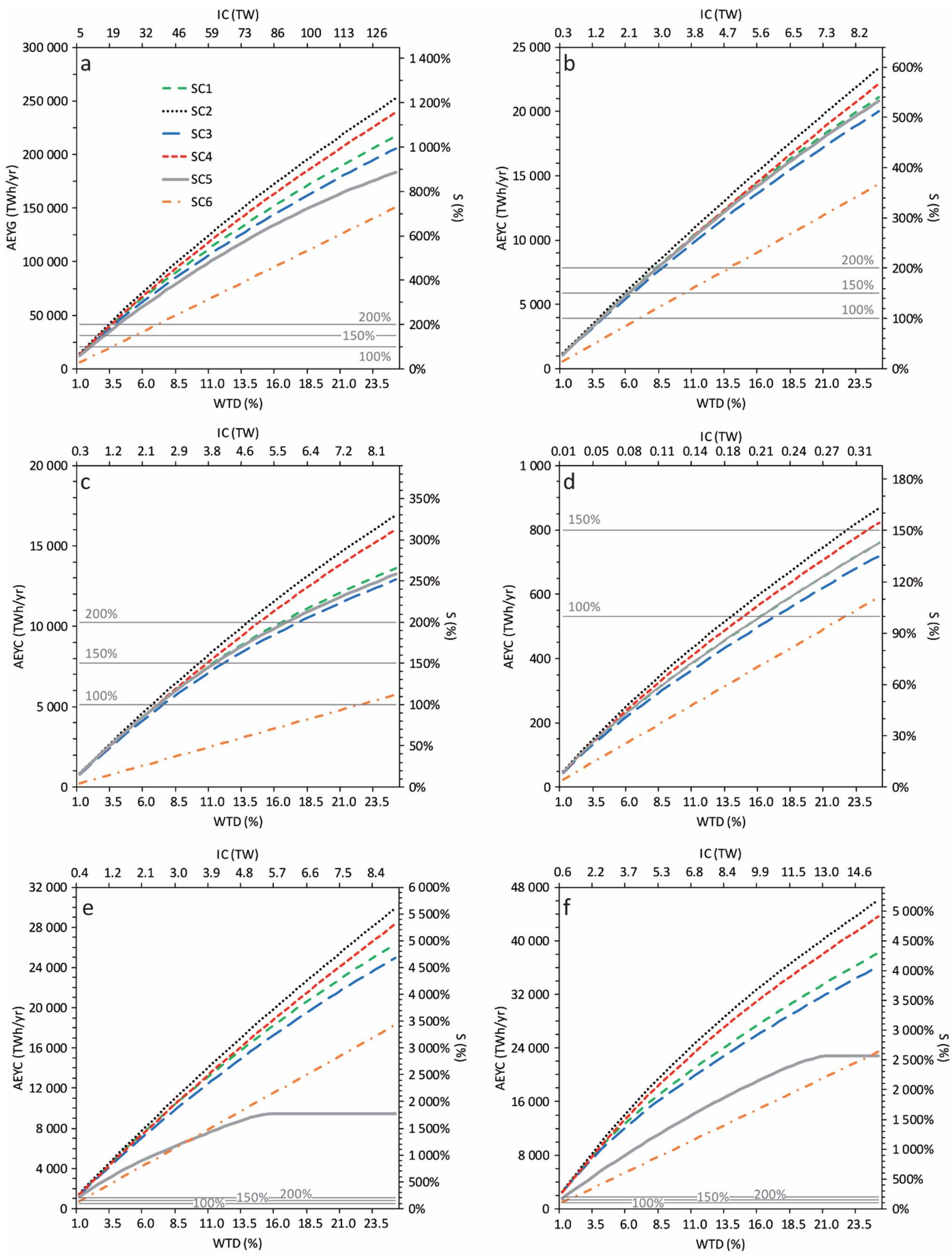

Fig. 10. Global average annual wind energy yield (*AEYG*), annual average wind energy yield per country (*AEYC*), share of electricity consumption of 2014 ($S = 100\%$) as a function of wind turbine density (*WTD*), and installed capacity (*IC*) for (a) the world, (b) the USA, (c) China, (d) Germany, (e) Canada, and (f) Russia.

consumption (Fig. 10d). Assuming a random siting of wind turbines (SC6), Germany's current electricity consumption can only be covered by *WTD* = 22.5% and *IC* = 0.29 TW.

In Canada, electricity consumption can easily be covered assuming *WTD* = 1% and *IC* = 0.36 TW in all scenarios (Fig. 10e). Excluding permafrost areas, only 15.5% of Canada's area remain for wind turbine installation (SC5). However, this still allows utilizing nearly 18 times more wind energy than Canada's current electricity consumption.

A similar situation can be found in Russia (Fig. 10f). By realizing wind energy at *WTD* = 1% and *IC* = 0.62 TW, the current Russian electricity consumption could be covered under all scenarios without any difficulty. Even though the assumption of SC5 reduces the area of Russia suitable for wind turbine installation to 21%, the remaining area would be sufficient to provide more than 25 times Russia's current electricity consumption.

In Fig. 11, the global *SR* pattern is shown for *WTD* = 2%. In Colombia, Chile, and Indonesia *SR* > 450%. In countries such as Greece, Turkey, Peru, Cameroon, and Papua New Guinea, *SR* > 400%. In these countries, wind turbines should be systematically sited in areas where *AEY* is high. In Australia, the USA, and Canada, *SR* varies between 162% and 190%. This indicates that systematic wind turbine siting could considerably increase *AEYC*. In Puerto Rico, Bahrain or Jamaica, effects of the wind turbine siting strategy are of minor importance (*SR* = 100%).

The available spatial resolution of the wind data prevented a more detailed analysis of *SR* at smaller spatial scales. Especially, in countries with complex terrain, the use of high-spatial resolution (e.g. 50 m × 50 m) wind speed data [44] would most probably lead to an increase of *SR* because the difference between the systematic SC1-related siting strategy and the random SC6-related siting increases.

Under SC1-SC5, global mean *CF* is always higher than under SC6, regardless of *WTD* (Fig. 12a). At *WTD* = 1.0% and *IC* = 5.4 TW, global *CF* varies between 0.26 (SC5) and 0.30 (SC2). This is due to the fact that under SC1-SC5 wind turbines are first installed at sites where *AEY* is highest. Therefore, a further increase in *WTD* reduces *CF* due to additional wind turbine installation at sites with lower *AEY*. This also entails that wind turbines, which are installed at a later expansion stage, always achieve lower *AEY* as wind turbines installed at an early expansion stage. For *WTD* = 4.0% and *IC* = 21.5 TW, *CF* would decrease to 0.22 (SC5) and 0.27 (SC2). The random wind turbine siting under SC6 ultimately results in global mean *CF* presenting mean *CF* of all non-restricted land areas (0.13), independent of *WTD*.

In the USA, average *CF* resulting from random wind turbine siting equals to 0.19 (Fig. 12b). Under SC1-SC5, the greatest decrease of *CF* occurs up to *WTD* = 3.5%. Over the entire *WTD* range, *CF* remains above 0.25.

In contrast, under SC6, average *CF* calculated for China is rather low (0.08) (Fig. 12c). All systematic installation scenarios result in considerably higher *CF* even at highest *WTD*. Under SC2, *CF* is highest over the simulated *WTD* range. Beginning with *WTD* > 6.5%, it is more efficient to install wind turbines under SC2 and SC4 than under SC1 and SC3.

Under SC6, average *CF* of Germany is 0.21 (Fig. 12d). This is much lower than *CF* under SC1-SC5, especially at low *WTD*. At *WTD* = 1.0% and *IC* = 0.01 TW, *CF* varies between 0.39 (SC3) and 0.43 (SC2) which means that *CF* under all systematic wind turbine installation scenarios is nearly twice as high as under SC6. At *WTD* = 25.0% and *IC* = 0.33 TW, *CF* decreases to approximately 0.25 in SC3.

At low *WTD*, *CF* calculated for Canada (Fig. 12e) and Russia (Fig. 12f) is about 0.45 under SC1-SC4. These high *CF* values result from large areas in the northern parts of Canada and Russia where the wind resource is abundant and allows for extensive wind energy utilization. However, excluding permafrost areas leads to a substantial reduction in *CF*. In Canada, *CF* reaches its minimum (0.19) at *WTD* = 15.5% under SC5 which is even below *CF* related to SC6. This implies that at *WTD* ≥ 15.5% maximum installed capacity is reached. In Russia, maximum installed capacity is reached at 21.0% with *CF* = 0.22 still being above *CF* related to SC6.

3.5. Limitations

The results obtained in this study are presented for installation scenarios under current conditions. However, the factors that determine wind energy utilization such as the wind resource, surface properties, and wind turbine technology are dynamic. It is clear that future changes of these factors imply changes of the future wind energy potential. Furthermore, the wind energy generation is compared to electricity consumption of 2014. However, electricity consumption strongly varies as a function of socio-economic variables including gross domestic product, energy imports and exports, and population. Moreover, the growing importance of demand side management also influences electricity consumption [45]. Thus, the estimated *S* values only reproduce the current technical wind energy potential to cover electricity consumption.

Other factors, which include economic and implementation restrictions were not considered in this study, also influence the utilization of wind energy. Among these factors are costs incurred from installation, long-distance electricity transmission, and storage.

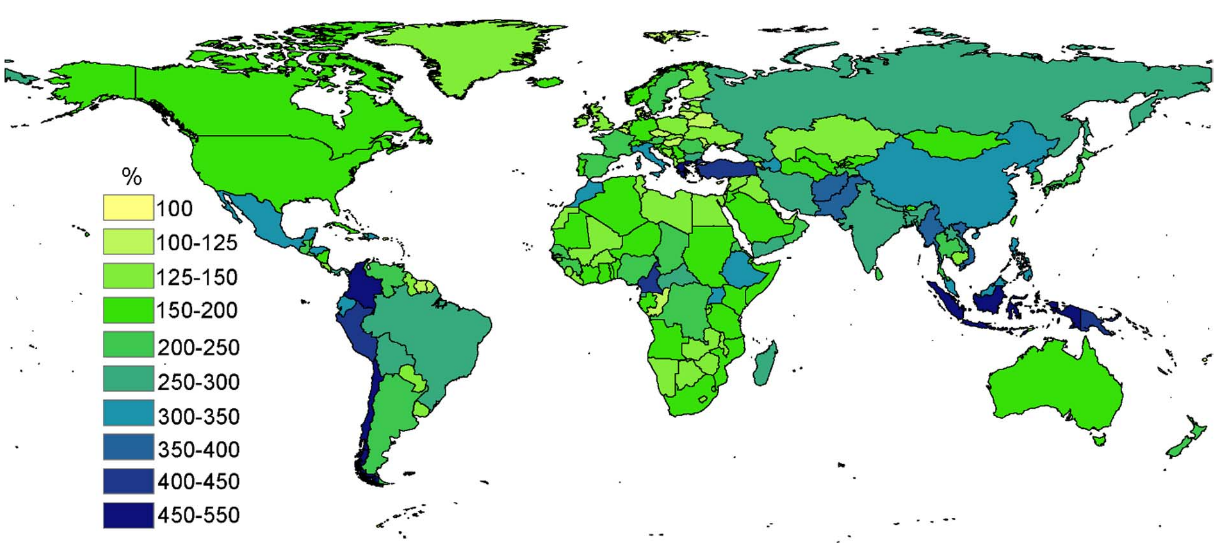

Fig. 11. Global pattern of the scenario ratio (*SR*).

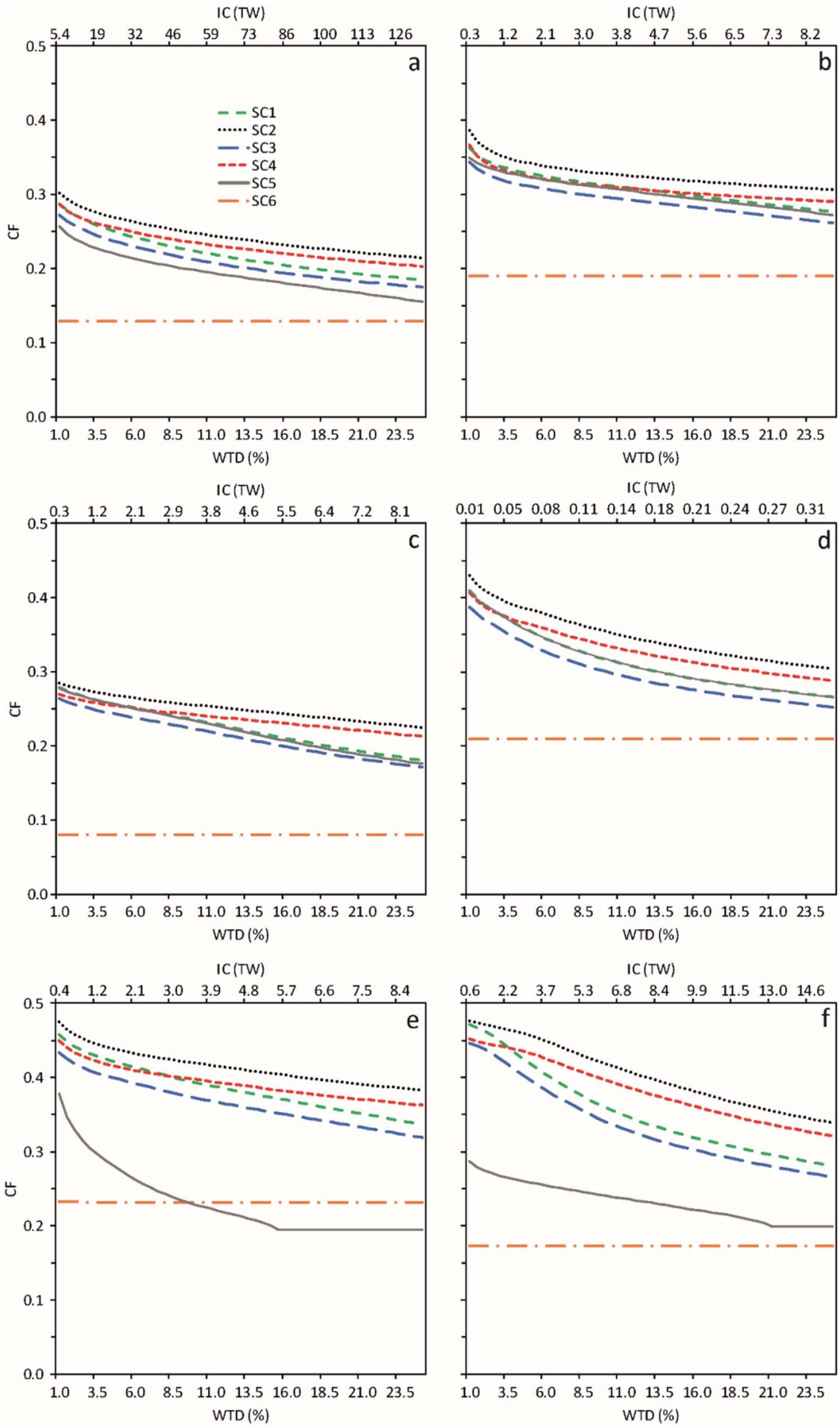

Fig. 12. Capacity factor (*CF*) as a function of wind turbine density (*WTD*) and installed capacity (*IC*) for (a) the world, (b) the USA, (c) China, (d) Germany, (e) Canada, and (f) Russia.

Furthermore, systematic wind turbine installation involves giving priority to wind energy development over other land uses. Conflicts with wildlife, sound and visual impacts caused by operating wind turbines might also limit the acceptance of efficiently harvesting wind energy.

4. Conclusions

The simulation results suggest that the current expansion rate of onshore wind energy is not sufficient to cover global electricity consumption in a reasonable timeframe. However, systematic wind turbine siting and electricity allocation, coordinated at national and international levels, could substantially improve the availability of wind energy. On the global scale, matching electricity consumption could be possible if all countries would install wind turbines at 2% of their area. It is furthermore reasonable to assume that the findings of this study help to prioritize areas at national and global scale which are especially suitable for wind energy utilization. The range of annual average wind energy yield per country estimates is assumed to be valuable information for decision support with respect to future development of wind energy expansion. Yet, the expansion of wind energy in the industrialized countries takes place under different conditions as in many developing countries. In a large number of developing countries, the construction of a functioning electricity grid and access to affordable modern energy services are still the greatest challenges [46]. By contrast, in many industrialized countries the conversion of electricity grids and the efficient integration of wind energy into the existing energy mix of must be improved.

To develop the proposed approach further, it is suggested to increase the spatial resolution of the analysis [47] and to include more subnational and regional features, constraints, and incentives into the scenarios.

Conflicts of interest

This research did not receive any specific grant from funding agencies in the public, commercial or not-for-profit sectors.

Appendix A. Supplementary material

Supplementary data associated with this article can be found, in the online version, at http://dx.doi.org/10.1016/j.enconman.2017.11.059.

References

[1] Ferguson R, Wilkinson W, Hill R. Electricity use and economic development. Energ Policy 2000;28:923–34.
[2] Energy information administration. U.S. Department of energy. Total electricity net consumption; 2017. https://www.eia.gov/beta/international/; [accessed 01.10.17].
[3] Organisation for economic co-operation and development. OECD factbook 2015–2016; 2017. http://statlinks.oecdcode.org/302015041p1g092.xls. [accessed 01.10.17].
[4] Burnham A, Han J, Clark CE, Wang M, Dunn JB, Palou-Rivera I. Life-cycle greenhouse gas emissions of shale gas, natural gas, coal, and petroleum. Environ Sci Technol 2011;46:619–27.
[5] Sunderland EM, Driscoll Jr CT, Hammitt JK, Grandjean P, Evans JS, Blum JD, et al. Benefits of regulating hazardous air pollutants from coal and oil-fired utilities in the United States. Environ Sci Technol 2016;50:2117–20.
[6] Höök M, Tang X. Depletion of fossil fuels and anthropogenic climate change—a review. Energy Policy 2013;52:797–809.
[7] Edenhofer O, Pichs-Madruga R, Sokona Y. Special Report Renewable Energy Sources (SRREN). Renewable energy sources and climate change mitigation. New York: Cambridge University Press, IPCC; 2012.
[8] Jacobson MZ, Masters GM. Exploiting wind versus coal. Science 2001;293:1438.
[9] He W, Ge SS. Vibration control of a nonuniform wind turbine tower via disturbance observer. IEEE ASME Trans Mechatron 2015;20:237–44.
[10] Leung DY, Yang Y. Wind energy development and its environmental impact: A review. Renew Sustain Energy Rev 2012;16:1031–9.
[11] World wind energy association. World wind market has reached 486 GW from where 54 GW has been installed last year; 2017. http://www.wwindea.org/wp-content/uploads/filebase/market_reports/Wind_Energy_Installations_2016.pdf. [accessed 02.10.17].
[12] Manwell JF, McGowan JG, Rogers AL. Wind energy explained: theory, design and application. England: John Wiley; 2009.
[13] Lu X, McElroy MB, Kiviluoma J. Global potential for wind-generated electricity. Proc Natl Acad Sci USA 2009;106:10933–8.
[14] Miller LM, Gans F, Kleidon A. Estimating maximum global land surface wind power extractability and associated climatic consequences. Earth Syst Dynam 2011;2:1–12.
[15] Gans F, Miller LM, Kleidon A. The problem of the second wind turbine – a note on a common but flawed wind power estimation method. Earth Syst Dynam Discuss 2010;1:103–14.
[16] Jacobson MZ, Archer CL. Saturation wind power potential and its implications for wind energy. Proc Natl Acad Sci USA 2012;109:15679–84.
[17] DeCarolis JF, Keith DW. The economics of large-scale wind power in a carbon constrained world. Energ Policy 2006;34:395–410.
[18] Langer K, Decker T, Roosen J, Menrad K. A qualitative analysis to understand the acceptance of wind energy in Bavaria. Renew Sustain Energy Rev 2016;64:248–59.
[19] Poli P, Hersbach H, Tan D, Dee D, Thepaut JN, Simmons A, et al. The data assimilation system and initial performance evaluation of the ECMWF pilot reanalysis of the 20th-century assimilating surface observations only (ERA-20C). ERA Report Series 2013;14:1–59.
[20] European centre for medium-range weather forecasts. ERA-20C daily; 2017. http://apps.ecmwf.int/datasets/data/era20c-daily/levtype=sfc/type=an/. [accessed 14.11.17].
[21] Poli P, Hersbach H, Dee DP, Berrisford P, Simmons AJ, Vitart F, et al. ERA-20C: An atmospheric reanalysis of the twentieth century. J Clim 2016;29:4083–97.
[22] Jung C. High spatial resolution simulation of annual wind energy yield using near-surface wind speed time series. Energies 2016;9:344.
[23] Jung C, Schindler D. Global analysis of the goodness-of-fit of wind speed distributions. Energy Convers Manage 2017;133:216–34.
[24] Jung C, Schindler D, Laible J, Buchholz A. Introducing a system of wind speed distributions for modeling properties of wind speed regimes around the world. Energy Convers Manage 2017;144:181–92.
[25] Marquardt DW. An algorithm for least-squares estimation of nonlinear parameters. J Soc Ind Appl Math 1963;11:431–41.
[26] Lydia M, Kumar SS, Selvakumar AI, Kumar GEP. A comprehensive review on wind turbine power curve modeling techniques. Renew Sustain Energy Rev 2014;30:452–60.
[27] Gamesa Corporación Tecnológica. Gamesa 5.0 MW innovating for reliability; 2015. http://www.gamesacorp.com/recursos/doc/productos-servicios/aerogeneradores/catalogo-g10x-45mw-eng.pdf. [accessed 01.10.17].
[28] ENERCON GmbH. E-126 EP4; 2016. http://www.enercon.de/en/products/ep-4/e-126-ep4/. [accessed 01.10.17].
[29] Vestas wind systems A/S. V112-3.45 MW™ at a glance; 2017. https://www.vestas.com/en/products/turbines/v112-3_45_mw#!about. [accessed 01.10.17].
[30] Siemens AG. Onshore direct drive wind turbine SWT-3.2-113; 2017. https://www.siemens.com/global/en/home/markets/wind/turbines/swt-3-2-113.html. [accessed 01.10.17].
[31] VENSYS energy AG. 2.5 MW Platform; 2017. http://www.vensys.de/energy-wAssets/docs/pdf-dateien-fuer-download/VENSYS-2-5MW-english.pdf. [accessed 28.03.17].
[32] Boccard N. Capacity factor of wind power realized values vs. estimates. Energ. Policy 2009;37:2679–88.
[33] Chang TP. Estimation of wind energy potential using different probability density functions. Appl Energy 2011;88:1848–56.
[34] Loveland TR, Reed BC, Brown JF, Ohlen DO, Zhu Z, Yang LWMJ, et al. Development of a global land cover characteristics database and IGBP DISCover from 1 km AVHRR data. Int J Remote Sens 2000;21:1303–30.
[35] International union for conservation of nature. The world database on protected areas (WDPA); 2014. https://www.iucn.org/theme/protected-areas/our-work/world-database-protected-areas. [accessed 01.10.17].
[36] Danielson JJ, Gesch DB. Global multi-resolution terrain elevation data 2010 (GMTED2010): U.S. Geological Survey. Open-File Report 2011;1073.
[37] Mentis D, Hermann S, Howells M, Welsch M, Siyal SH. Assessing the technical wind energy potential in Africa a GIS-based approach. Renew Energy 2015;83:110–25.
[38] Gruber S. Derivation and analysis of a high-resolution estimate of global permafrost zonation. Cryosphere 2012;6:221–33.
[39] University of Zurich, Department of Geography; 2017. http://www.geo.uzh.ch/microsite/cryodata/pf_global/. [accessed 01.10.17].
[40] Barthelmie RJ, Jensen LE. Evaluation of wind farm efficiency and wind turbine wakes at the Nysted offshore wind farm. Wind Energy 2010;13:573–86.
[41] Petković D, Pavlović NT, Ćojbašić Ž. Wind farm efficiency by adaptive neuro-fuzzy strategy. Int J Elec Power 2016;81:215–21.
[42] Conroy N, Deane JP, Gallachóir BPÓ. Wind turbine availability: Should it be time or energy based? – A case study in Ireland. Renew Energy 2011;36:2967–71.
[43] Brew-Hammond A. Energy access in Africa: Challenges ahead. Energ Policy 2010;38:2291–301.
[44] Jung C, Schindler D. Statistical modeling of near-surface wind speed: A case study from Baden-Wuerttemberg (Southwest Germany). Austin J Earth Sci 2015;2:1–11.
[45] Ardakani FJ, Ardehali MM. Novel effects of demand side management data on accuracy of electrical energy consumption modeling and long-term forecasting. Energy Convers Manage 2014;78:745–52.
[46] Winkler H, Simões AF, La Rovere EL, Alam M, Rahman A, Mwakasonda S. Access and affordability of electricity in developing countries. World Dev 2011;39:1037–50.
[47] Grau L, Jung C, Schindler D. On the annual cycle of meteorological and geographical potential of wind energy: a case study from Southwest Germany. Sustainability 2017;9:1169.